

2012-01-30

Evanescent Field Coupling Between Two Parallel Close Contact SMS Fiber Structures

Qiang Wu

Technological University Dublin, qiang.wu@tudublin.ie

Youqiao Ma

Technological University Dublin

Jinhui Yuan

University of Posts and Telecommunications, Beijing

See next page for additional authors

Follow this and additional works at: <https://arrow.tudublin.ie/engscheceart>



Part of the [Electromagnetics and Photonics Commons](#), and the [Systems and Communications Commons](#)

Recommended Citation

Wu, Q., Ma, Y. Yuan, J., Semenova, Y, Wang, P.: Evanescent field coupling between two parallel close contact SMS fiber structures. *Optics Express*, Vol.20, 3, 2012, pg. 3098-3109. doi:10.1364/OE.20.003098

This Article is brought to you for free and open access by the School of Electrical and Electronic Engineering (Former DIT) at ARROW@TU Dublin. It has been accepted for inclusion in Articles by an authorized administrator of ARROW@TU Dublin. For more information, please contact arrow.admin@tudublin.ie, aisling.coyne@tudublin.ie, vera.kilshaw@tudublin.ie.

Authors

Qiang Wu, Youqiao Ma, Jinhui Yuan, Yuliya Semenova, Pengfei Wang, Chongxiu Yu, and Gerald Farrell

Evanescence field coupling between two parallel close contact SMS fiber structures

Qiang Wu,^{1,*} Youqiao Ma,¹ Jinhui Yuan,² Yuliya Semenova,¹ Pengfei Wang,¹
Chongxiu Yu,² and Gerald Farrell¹

¹Photonics Research Centre, School of Electronic and Communications Engineering, Dublin Institute of Technology, Kevin Street, Dublin 8, Ireland

²Laboratory of Information Photonics and Optical Communications, Beijing University of Posts and Telecommunications, Ministry of Education, P.O. Box 72 (BUPT), Beijing 100876, China
* qiang.wu@dit.ie

Abstract: We proposed a novel optical coupling technique based on two parallel singlemode-multimode- singlemode (SMS) fiber structures. This technique utilizes one SMS structure to excite multiple cladding modes within an output singlemode fiber. The excited multiple cladding modes will be coupled to the input SMF in the second SMS structure by placing the two SMS fiber structures in parallel and in close contact each other. The coupled cladding modes will be re-coupled to a guided core mode by the second SMS fiber structure. Theoretical analysis for such technique was provided and experimentally we have achieved a pass band spectral response with an extinction ratio higher than 20 dB and a maximum coupling efficiency of 5.9%.

©2012 Optical Society of America

OCIS codes: (060.2340) Fiber optics components; (060.1810) Buffers, couplers, routers, switches, and multiplexers; (060.2330) Fiber optics communications.

References and links

1. M. J. Kim, Y. M. Jung, B. H. Kim, W. T. Han, and B. H. Lee, "Ultra-wide bandpass filter based on long-period fiber gratings and the evanescent field coupling between two fibers," *Opt. Express* **15**(17), 10855–10862 (2007).
2. P. K. Lam, A. J. Stevenson, and J. D. Love, "Bandpass spectra of evanescent couplers with long period gratings," *Electron. Lett.* **36**(11), 967–969 (2000).
3. Q. Liu, K. S. Chiang, and Y. Q. Liu, "Analysis of six-port optical fiber couplers based on three parallel long-period fiber gratings," *J. Lightwave Technol.* **26**(18), 3277–3286 (2008).
4. Y. Q. Liu, K. S. Chiang, Y. J. Rao, Z. L. Ran, and T. Zhu, "Light coupling between two parallel CO₂-laser written long-period fiber gratings," *Opt. Express* **15**(26), 17645–17651 (2007).
5. Y. M. Jung, G. Brambilla, G. S. Murugan, and D. J. Richardson, "Optical racetrack ring-resonator based on two U-bent microfibers," *Appl. Phys. Lett.* **98**(2), 021109 (2011).
6. Z. H. Hong, X. W. Li, L. J. Zhou, X. W. Shen, J. G. Shen, S. G. Li, and J. P. Chen, "Coupling characteristics between two conical micro/nano fibers: simulation and experiment," *Opt. Express* **19**(5), 3854–3861 (2011).
7. X. S. Jiang, L. M. Tong, G. Vienne, X. Guo, A. Tsao, Q. Yang, and D. Yang, "Demonstration of optical microfiber knot resonators," *Appl. Phys. Lett.* **88**(22), 223501 (2006).
8. Y. Wu, X. Zeng, C. L. Hou, J. Bai, and G. G. Yang, "A tunable all-fiber filter based on microfiber loop resonator," *Appl. Phys. Lett.* **92**(19), 191112 (2008).
9. Q. Wu, Y. Semenova, P. Wang, and G. Farrell, "High sensitivity SMS fiber structure based refractometer--analysis and experiment," *Opt. Express* **19**(9), 7937–7944 (2011).
10. L. B. Soldano and E. C. M. Pennings, "Optical multi-mode interference devices based on self-imaging: principles and applications," *J. Lightwave Technol.* **13**(4), 615–627 (1995).
11. Q. Wu, Y. Semenova, J. Mathew, P. Wang, and G. Farrell, "Humidity sensor based on a single-mode hetero-core fiber structure," *Opt. Lett.* **36**(10), 1752–1754 (2011).
12. W. S. Mohammed, A. Mehta, and E. G. Johnson, "Wavelength tunable fiber lens based on multimode interference," *J. Lightwave Technol.* **22**(2), 469–477 (2004).
13. Q. Wu, A. M. Hatta, P. Wang, Y. Semenova, and G. Farrell, "Use of a bent single SMS fiber structure for simultaneous measurement of displacement and temperature sensing," *IEEE Photon. Technol. Lett.* **23**(2), 130–132 (2011).
14. S. M. Tripathi, A. Kumar, R. K. Varshney, Y. B. P. Kumar, E. Marin, and J. P. Meunier, "Strain and temperature sensing characteristics of single-mode-multimode- single-mode structures," *J. Lightwave Technol.* **27**(13), 2348–2356 (2009).

15. Q. Wu, Y. Semenova, B. B. Yan, Y. Q. Ma, P. Wang, C. X. Yu, and G. Farrell, "Fiber refractometer based on a fiber Bragg grating and single-mode-multimode-single-mode fiber structure," *Opt. Lett.* **36**(12), 2197–2199 (2011).
16. H. Kogelnik and R. V. Schmidt, "Switched directional couplers with alternating $\Delta\beta$," *IEEE J. Quantum Electron.* **12**(7), 396–401 (1976).
17. K. S. Chiang, F. Y. M. Chan, and M. N. Ng, "Analysis of two parallel long-period fiber gratings," *J. Lightwave Technol.* **22**(5), 1358–1366 (2004).

1. Introduction

Optical couplers based on parallel long period gratings (LPG) written in single mode fibers have been extensively investigated recently [1–4]. This technique utilizes the fact that an LPG can couple light from the guided core mode to a selected cladding mode and can also couple light from a cladding mode to a guided core mode. Another approach is based on tapered optical microfiber which utilizes evanescent field coupling within the tapered region [5–8]. However both of these techniques suffer from the disadvantage of high cost due to the relatively complex fabrication processes involved. Compared to these techniques, a singlemode-multimode-singlemode (SMS) fiber structure offers low cost and ease of fabrication and has been used for temperature, strain and refractive index (RI) sensing [9–14]. In an SMS fiber structure multimode interference occurs within the multimode fiber (MMF) section when light is injected from a singlemode fibre (SMF) into the MMF. When the light is coupled again to the output singlemode fibre (SMF), it will excite both core and cladding modes propagating within the SMF. The excitation of both core and cladding modes can be useful, for example if the SMS fiber structure is followed by a fiber Bragg grating (FBG), both core and cladding mode Bragg wavelengths will be guided to the SMF core and such a structure can be used as an RI sensor [15]. In this paper we propose and investigate a novel fiber-to-fiber coupling technique based on two parallel SMS fiber structures by utilizing the process whereby cladding modes are excited in one SMS structure and re-coupled to a core mode in a second SMS fiber structure. A theoretical analysis based on the proposed configuration is provided, along with experimental verification.

2. Theoretical background

The fiber configuration for the proposed coupling technique is shown in Fig. 1.

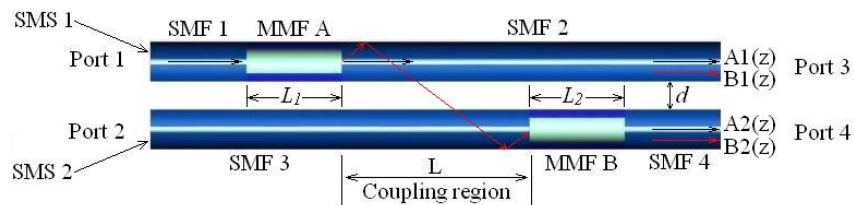


Fig. 1. Configuration of the fiber-to-fiber coupling technique based on two parallel SMS fiber structures.

In Fig. 1, there are two separate SMS fiber structures which are constructed from coating stripped SMF and MMF by fusion splicing. Both the SMF and MMF fibers have a step index profile. While the coating is stripped from a short length of the fibers used in order to facilitate fabrication, all the connecting input and output fibers retain their polymer coatings. When the two SMS structures are physically apart (a large value for the separation d in Fig. 1) then they behave as expected, for example for SMS 1, when light is injected from SMF 1 into MMF A, multiple modes will be excited and will propagate within MMF A and then excite both core and cladding modes in SMF 2. The core mode within the SMF 2 will propagate with minimal energy loss but the cladding modes will dissipate due to absorption when the modes reach the portion of the fiber with unstripped polymer. However if the two SMS fiber structures are placed close to each other, ideally in physical contact, and assuming light is injected into Port 1, then the cladding modes in SMF 2 will be coupled to SMF 3 due to evanescent field coupling between the two parallel fibers SMF 2 and SMF 3. The coupled

cladding modes in SMF 3 will enter the fiber core of MMF B, which in turn will excite a guided core mode in SMF 4 and hence the coupled light will be transmitted to port 4.

Assuming the amplitudes of the core and cladding modes within the SMF are $A(z)$ and $B(z)$ respectively and MMF A and B are the same type of fiber but with different lengths L_1 and L_2 , then the field after a propagation distance L_1 within MMF A can be written as:

$$A_1(r, L_1) = \sum_{m=1}^M b_m \Psi_m(r) \exp(j\beta_m L_1) \quad (1)$$

where $\Psi_m(r)$ is the field profile within MMF (both A and B) corresponding to m^{th} eigenmode, β_m is the propagation constant of the m^{th} eigenmode within the MMF, M is the total number of modes propagating within the MMF and b_m is the excitation coefficient for each mode which can be expressed as:

$$b_m = \frac{\int_0^\infty \Omega(r) \Psi_m(r) r dr}{\int_0^\infty \Psi_m(r) \Psi_m(r) r dr} \quad (2)$$

where $\Omega(r)$ is the eigenmode of the SMF 1 which is the input to the MMF A. At the output of MMF A, the light will be coupled to both core and cladding modes within SMF 2 and the excitation coefficient for each mode b'_n can be expressed as:

$$b'_n = \frac{\int_0^\infty A_1(r, L_1) \Phi_n(r) r dr}{\int_0^\infty \Phi_n(r) \Phi_n(r) r dr} \quad (3)$$

where $\Phi_n(r)$ is n^{th} eigenmode within SMF 2 ($n=1$ represents the core mode and $n>1$ represents cladding modes). The field of the n^{th} cladding mode at a position L_1 within the SMF 2 can thus be written as:

$$B_{1_n}(r, L_1) = b'_n \Phi_n(r) \quad (4)$$

The mode fields above are normalised as

$$\int_0^\infty \Omega(r) \Omega(r) r dr = \int_0^\infty \Psi_m(r) \Psi_m(r) r dr = \int_0^\infty \Phi_n(r) \Phi_n(r) r dr = 1 \quad (5)$$

Over the length of the coupling region, assuming the two parallel fibers are identical, then there is no mismatch between the propagation constants of the two fibers and hence the amplitudes of the n^{th} cladding modes B_{1_n} and B_{2_n} at position $L_1 + L$ can be expressed as [16]:

$$B_{1_n}(r, L_1 + L) = B_{1_n}(r, L_1) \cos(C_n L) \quad (6)$$

$$B_{2_n}(r, L_1 + L) = -j B_{1_n}(r, L_1) \sin(C_n L) \quad (7)$$

where C_n is the evanescent field coupling coefficient of the n^{th} cladding mode between the two parallel fibers which can be approximately expressed as [17]:

$$C_n = \frac{\sqrt{2\Delta} U_n^2 K_0 [W_n (2 + d/a_0)]}{a_0 V_n^3 K_1^2(W_n)} \quad (8)$$

where a_0 is the radius of the fiber cladding and d (shown in Fig. 1) is the separation between the two parallel fibers, K_0 and K_1 are the modified Bessel functions, $\Delta = \frac{n_c^2 - n_s^2}{2n_c^2}$ is the relative refractive index difference between the cladding (n_c) and surrounding medium (n_s). $U_n = \frac{2\pi a_0}{\lambda} \sqrt{n_c^2 - N_n^2}$, $V_n = \frac{2\pi a_0}{\lambda} \sqrt{n_c^2 - n_s^2}$ and $W_n = \frac{2\pi a_0}{\lambda} \sqrt{N_n^2 - n_s^2}$ are the normalized parameters and N_n is the effective refractive index of the n^{th} cladding mode.

The cladding modes in SMF 3 will then be coupled to core modes propagating within MMF B which can be expressed as follows:

$$E(r, L_1 + L + L_2) = \sum_{m=1}^M c_m \Psi_m(r) \exp(j\beta_m L_2) \quad (9)$$

where

$$c_m = \sum_{n=2}^N \frac{\int_0^{\infty} B_{2n}(r, L_1 + L) \Psi_m(r) r dr}{\int_0^{\infty} \Psi_m(r) \Psi_m(r) r dr} \quad (10)$$

The core modes transmitted within MMF B will be coupled to the core mode within SMF 4 which will propagate within the SMF 4 core. The amplitude of the core mode within SMF 4 can thus be expressed as:

$$A_2(r, L_1 + L + L_2) = \frac{\int_0^{\infty} E(r, L_1 + L + L_2) \Omega(r) r dr}{\int_0^{\infty} \Omega(r) \Omega(r) r dr} \quad (11)$$

By numerically solving the above equations, the characteristics of the light coupled from port 1 to port 4 can be calculated.

3. Numerical simulations

Simulation was firstly carried out to investigate the spectral response of the SMS fiber structures with two different MMF lengths. Figures 2(a) and 2(b) shows examples of the simulated transmission spectra for the guided core mode and selected cladding modes within SMF at different MMF lengths. In this simulation example, the SMF has core and cladding diameters of 8.3 and 125 μm and refractive indices of 1.4504 and 1.447 respectively and the surrounding medium is assumed to be air. The MMF has core and cladding diameters of 50 and 125 μm and refractive indices of 1.4446 and 1.4271 respectively and the lengths of the MMF sections are 9.7 and 10.6 mm respectively.

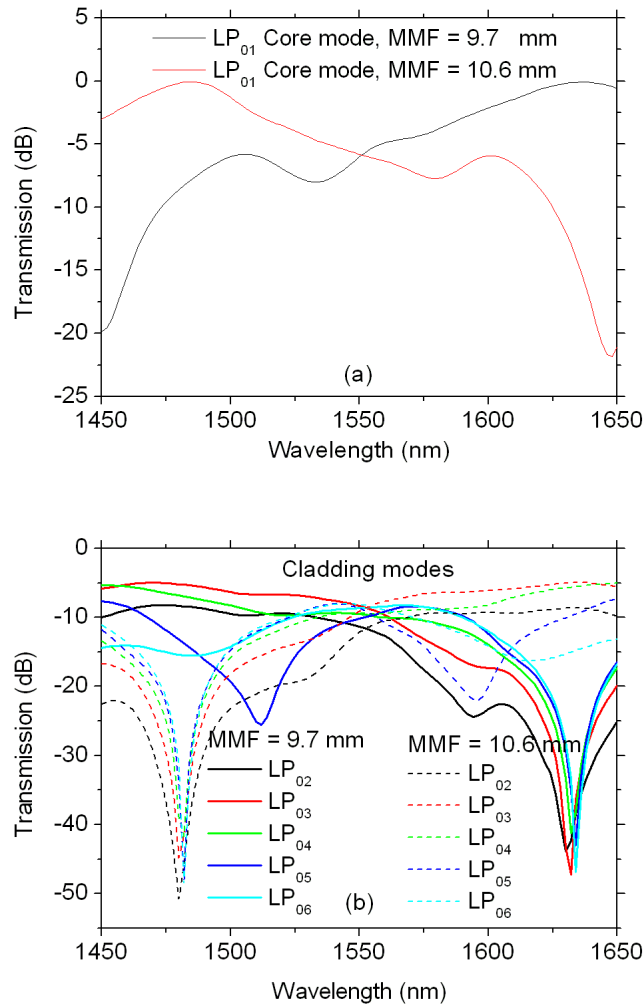


Fig. 2. Simulated transmission spectra for (a) LP_{01} core mode and (b) LP_{02-06} cladding modes within SMF in the SMS structure with different MMF lengths.

Figure 2(a) shows that for both MMF lengths, the guided core mode has a minimum loss less than 0.1 dB at a particular wavelength, corresponding to the self-imaging condition for each particular SMS fiber structure [7,8]. Figure 2(b) shows that the cladding modes each have different spectral responses vs. wavelength, and have minimum power at the peak wavelength corresponding to the self-imaging condition for the core mode. Since these cladding modes have different propagation constants, and hence different effective refractive indices, the result is a difference in the coupling coefficient for each mode. Figure 3 shows the simulated coupling coefficients for LP_{02-10} cladding modes between two close contact SMFs. In this simulation, we assume the RI of the surrounding medium is 1.44 and the separation between the two SMFs is zero ($d=0$).

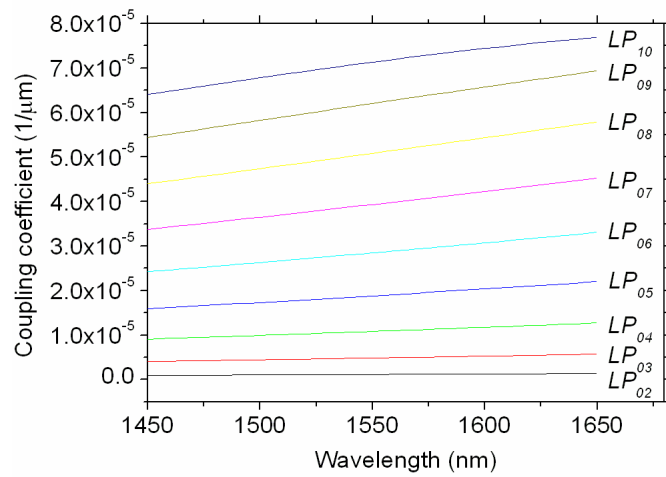


Fig. 3. Calculated coupling coefficients between two parallel SMFs for LP₀₂₋₁₀ cladding modes.

Figure 3 shows that a higher order mode has a larger coupling coefficient and that the coupling coefficient is wavelength dependant – for the same order cladding mode the coupling coefficient is larger at a longer wavelength. All the coupled cladding modes will be re-coupled to the SMF 4 core mode through MMF B. The simulated spectral response of the coupling between two SMS fiber structures is shown in Fig. 4. In this simulation we assume the two fibers are in perfect contact ($d=0$).

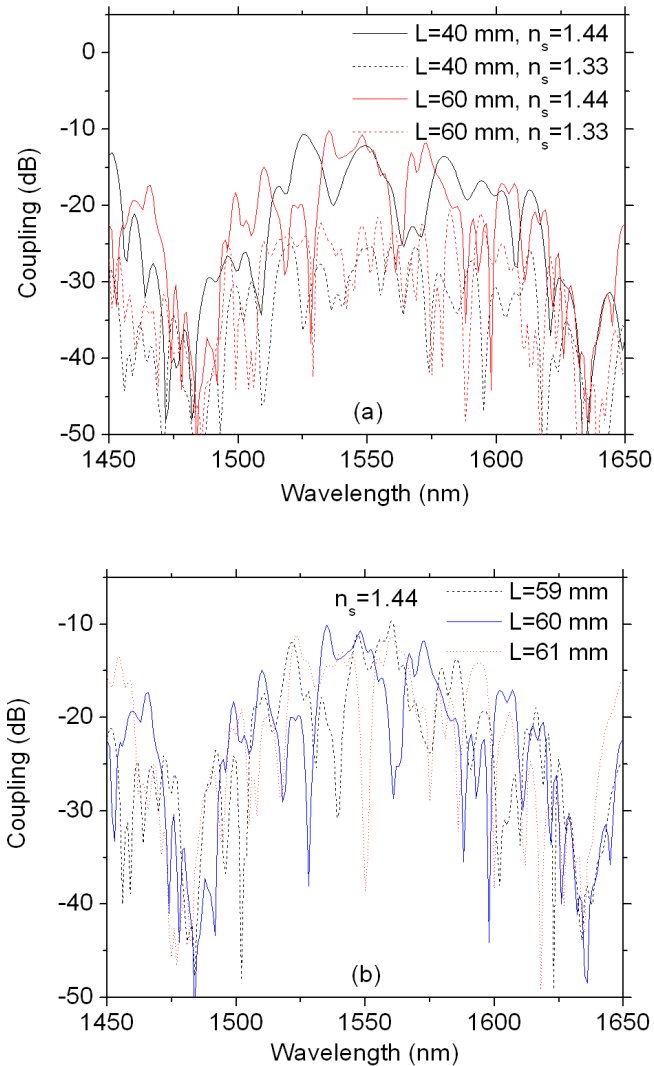


Fig. 4. Calculated coupling from Port 1 to Port 4 at different coupling lengths and SRI.

Figure 4(a) shows that when the light is injected from Port 1, the light is coupled to Port 4 and the coupling efficiency increases as the surrounding refractive index (SRI) increases from 1.33 to 1.44. The coupling efficiency and the spectral response change in a complex fashion as either the SRI or the coupling length L change. Figure 4(b) shows that at the same SRI value, even with a coupling length difference of only 1 mm, the coupled spectral response is significantly different. The reason is that the coupling coefficients for each of the cladding modes are significantly different as shown in Fig. 3. Both the SRI and coupling length will significantly influence the coupling efficiency for each mode, the result is that the final light interference between these coupled cladding modes changes in a complex fashion.

As is well known in practice it is very difficult to consistently achieve an ideal contact ($d = 0$) between two fibers. Investigations for the influence of separation distances d on the coupling were carried out as shown in Fig. 5.

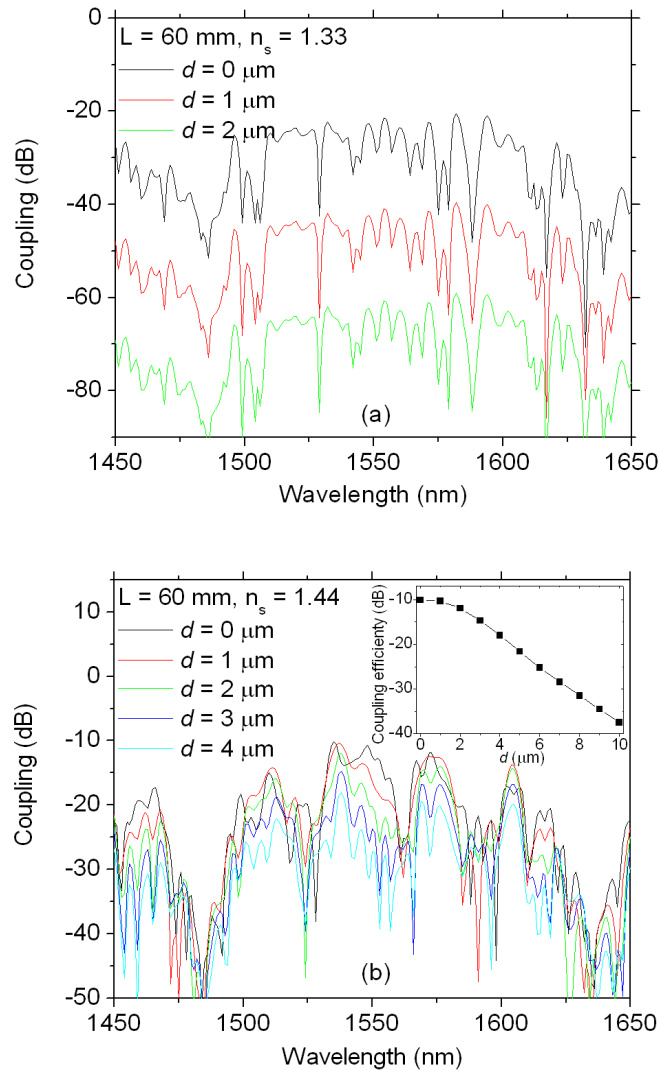


Fig. 5. Calculated influence of separation d on the coupling from Port 1 to Port 4 with coupling length $L = 60$ mm at two different SRI conditions (a) $n_s = 1.33$ and (b) $n_s = 1.44$.

For lower values of the SRI, $n_s = 1.33$, Fig. 5(a) shows that the influence on the coupling efficiency of a change of 1 μm in the separation d is significant: the coupling efficiency decreases by 19.2 dB. However as the SRI value n_s gets closer to the cladding refractive index of the fiber, the influence of separation d is much smaller as shown in Fig. 5(b). The inset in Fig. 5(b) shows that even with a larger SRI value of 1.44, larger values of the fiber separation d will nevertheless have a significant influence on the coupling efficiency which decreases from -10.1 to -37.5 dB as fiber separation d increases from 0 to 10 μm .

4. Experimental verification

Experiments based on the above coupling technique were carried out. In the experiments, the two SMS fiber structures were fabricated by fusion splicing SMF with MMF lengths of 10.8 and 10.0 mm respectively. The SMF used was conventional SMF28 fabricated by Corning and the MMF had a core diameter of 50 ± 1 μm . Both fibers have step index profiles. The

normalised transmission spectra for the two SMS fiber structures when they are completely separated are shown in Fig. 6.

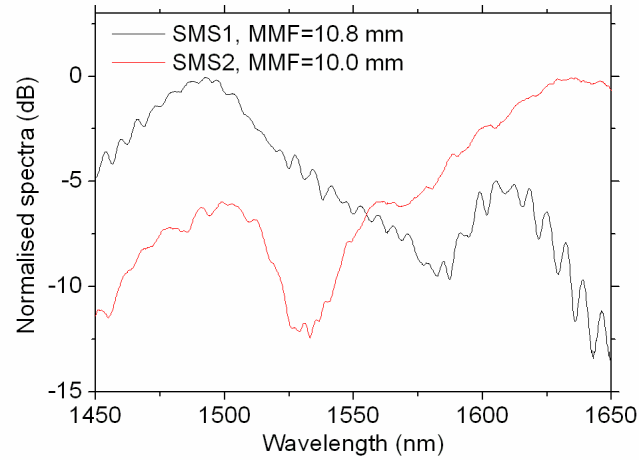


Fig. 6. Normalised transmission spectral responses of the two SMS fiber structures when separated.

Close physical contact between the two SMS fibre structures is arranged in free space over a contact region with a length of 12 cm. The fibres are pre-strained and aligned side-by-side with each other using V-grooves at either end of the 12 cm contact region.

Experiments were firstly carried out to investigate the influence of coupling length by injecting light at Port 1, with water as a surrounding liquid (SRI value of 1.334) but with different coupling lengths L circa 56 and 41 mm as shown in Fig. 7(a). For comparison purposes the simulated results with $L = 55.8$ and 40.5 mm are also presented in Fig. 7(a). In the simulation, the separation between two SMS fiber structures is set to zero, and all the other parameters are the same as above.

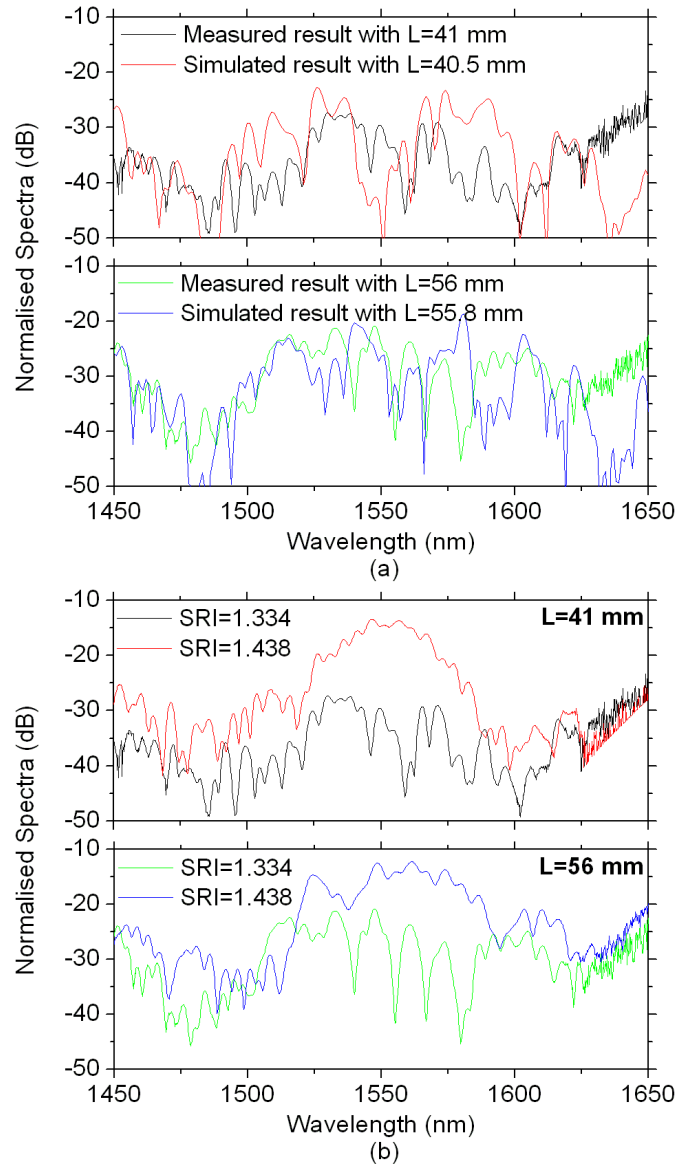


Fig. 7. (a) Comparison between simulation and experimental results for an SRI = 1.334 and (b) measured results at two different SRIs of 1.334 and 1.438 with different coupling lengths $L = 41$ and 56 mm.

Figure 7(a) confirms that when light is injected at Port 1, a portion of the input light is coupled from SMS 1 to Port 4 of SMS 2 because of the coupling of the cladding modes from SMF 2 in SMS 1 to the guided core mode in SMF 4 in SMS 2 by MMF B. It can be seen that with different coupling lengths, the coupling efficiency is different and the spectral response changes in a complex fashion as the coupling length L changes. Figure 7(a) also shows that the simulation results have a good match with the experimental results. The divergence between simulation and experiments is due to the differences in the fiber parameters (such as MMF lengths, RI of core and cladding, coupling length) used in the simulations along with variations in the value of the SRI and perturbations of the gap between the two structures.

To investigate the influence of SRI, another SRI matching liquid which consisted of a mixture of water and dimethyl sulfoxide was used. The refractive index of the mixed liquid is found from an Abbe 5 refractometer to be 1.438. The measured spectral response of the coupling between two SMS fiber structures was shown in Fig. 7(b).

Figure 7(b) shows that the coupling efficiency increases as the SRI value increases from 1.334 to 1.438 and the maximum efficiency is 5.9% (-12.3 dB). In both cases with L circa 41 and 56 mm, the spectral response has a band pass characteristic with typical extinction ratios higher than 20 dB. These results indicate that the SMS structure based coupling technique has potential applications in band pass filters and optical add-drop multiplexers in coarse wavelength division multiplexed optical communication systems.

The spectral response at Port 3 was also measured and was found to be the same as that shown in Fig. 6 and hence is not shown in Fig. 7.

Other input/output port combinations were also investigated. As expected light injected into Port 4 and detected at Port 1 has a similar spectral response to the Port 1 to Port 4 case above. The light injected from Port 2 to 3 was also investigated and our experimental result shows that there is no output power at Port 3. This is because although there are cladding modes coupled from SMF 4 to SMF 2 after light is transmitted through MMF B in SMS 2, the coupled cladding modes do not transit through the other MMF to be re-coupled to the guided core mode in SMF 2. These coupled cladding modes in SMF 2 will therefore dissipate due to absorption by unstripped polymer coating on the SMF.

It is noted that the length of the MMF has a significant influence on the transmission spectral response of the SMS fibre structure. In our experiments, we have found that a 100 micron variation in MMF length will introduce a circa 25 nm wavelength shift in the transmission spectra. However we can neglect the effect of length variations since the novel fabrication technique used can easily achieve better than one micron MMF length accuracy, thus ensuring that the fabrication of an SMS fibre structure is highly reproducible.

5. Conclusion and discussion

In conclusion, a novel fiber-to-fiber coupling technique based on evanescent-field coupling between two parallel SMS fiber structures was proposed. A theoretical analysis and experimental demonstration for such a coupling technique was provided. Experimental results show that the coupling has the characteristics of a pass band spectral response with an extinction ratio higher than 20 dB. Unlike fiber-to-fiber coupling based on parallel LPGs in which only one cladding mode is excited by the LPG, there are multiple cladding modes excited by the MMF in the SMS structure. The prediction of the coupled spectral response is more difficult than that for a coupling technique based on parallel LPGs since there are a larger number of cladding modes with different coupling coefficients, but the interference between multiple cladding modes potentially offers the possibility to customise the coupled spectrum, by a suitable selection of parameters. The transmission and coupling of multiple SMF cladding modes is influenced by a number of factors such as core diameters and refractive indices of the SMF and MMF, coupling length L and the SRI values and hence the characteristics of the spectral response are complex. In order to optimize the structure, an in-depth theory for the parallel SMS fiber structures should be developed. Experimentally we have achieved a maximum coupling efficiency of 5.9%. While this value is low, it is nevertheless an indication that coupling can take place and with further optimisation, the coupling efficiency could be improved. For example, it is well known that self-imaging phenomenon in an SMS fiber structure means that in theory there is no power loss on re-coupling for some wavelengths [10]. Since the proposed structure in this paper is based on two SMS fiber structures, it is possible to achieve improved operation for our proposed structure using optimized values for the diameter and length of MMFs, coupling length L and SRI, etc, all of which will significantly improve the coupling efficiency.

It should be pointed out that the technique proposed in this paper is sensitive to both the magnitude of the gap between the two parallel fiber structures and to variations in the coupling length. Our simulation shows that if the coupling length variation is below a value of

50 microns, there is no significant change for the spectral response. Compare to the coupled LPG technique, our proposed technique has a relatively low extinction ratio. This is possibly due to the fact that there are multiple cladding modes excited which interfere with each other and make it very difficult to achieve a relatively high extinction ratio.

Acknowledgment

This work was supported by Science Foundation Ireland under grant no. 07/SK/I1200, 11/TIDA/B2051, 07/SK/I1200-STTF11, 07/SK/I1200-ISTTF11; Open Fund of State Key Laboratory of Information Photonics and Optical Communications (Beijing University of Posts and Telecommunications), P. R. China; Dublin Institute of Technology under the Fiosraigh Research Scholarship; Irish Research Council for Science, Engineering and Technology; and Marie-Curie Actions under FP7.